AN UNSUPERVISED IMAGE ENDMEMBER DEFINITION APPROACH

A. Greiwe

University of Osnabrueck, Institute for Geoinformatics and Remote Sensing (FZG), Osnabrueck, Germany. email: agreiwe@igf.uni-osnabrueck.de

ABSTRACT

Multisensor Image Datasets are increasingly used for several remote sensing studies of urban areas in the last years. In recent studies the author developed a decision based data fusion approach for the analysis of spatial and spectral high resolution image data (i). It could be shown, that the inclusion of hyperspectral image data increases the classification accuracy significantly. As a precondition for the analysis of hyperspectral image data, the set of material reference spectra – often called image endmember - has to be defined. The process of endmember definition depends on the type of hyperspectral data analysis whether for unmixing or material detection approaches. For unmixing approaches like the Mixture Tuned Matched Filtering (MTMF), several autonomous endmember selection approaches like PPI or N-FINDR have been developed. These algorithms detect those pixels that define the convex hull of the n-dimensional feature space of hyperspectral image data. This leads to endmember that express 'spectral extreme' features.

However, these endmember definition approaches are not in every use-case suitable for material detection. Algorithms like the Spectral Angle Mapper (SAM), which was used in the author's data fusion approach described above, determine the spectral similarity between a pixel's spectra and a given endmember. In contrast to endmembers defining 'spectral extreme' features, SAM needs endmember representing the mean spectra of a material class in order to produce best possible results between spectral similar material classes. The objective of this work is the development and implementation of a non superivised image endmember definition approach for material detection approaches like SAM.

In a first step, in order to filter mixed-spectra, homogenous areas in the hyperspectral image data are selected by a GIS-overlay of image segments that were derived by a segmentation of high spatial resolution orthophotos. Pixel of the hyperspectral image data, that are completely included (within N4 or N8 neighborhood) in these segments, are marked as candidates for a endmember definition. Afterwards, the spectral correlation is used to calculate the spectral similarity between the candidates. At n given candidates, the n x n correlation matrix of all candidates is introduced as new feature space that expresses spectral similarity between the candidates. Candidates with similar spectral behaviour are grouped by a density based cluster algorithm and the mean spectra of each cluster is stored in a spectral library for further processing.

As a proof of principle, the proposed approach is used for the definition of several endmember in an urban test site. First results show a correct distinction between materials like concrete (red pavements), clay (red or brown rooftops), gravel, asphalt, and metal rooftops (copper, zinc).

INTRODUCTION

Hyperspectral image data contains - in contrast to multispectral image data - a huge amount of narrow bands which lead to an high dimensional "image data cube". To process these large data, special classification algorithms, whether for spectral unmixing or for material detection purposes, have been developed. Material detection algorithms like the Spectral Angle Mapper (SAM) calculate a deterministic value to express the spectral similarity of a pixel's spectra to a given reference. Unmixing approaches like the Mixture Tuned Matched Filtering (MTMF) determine for a measured spectrum the abundance fraction of a given reference spectrum. In both cases, the term "endmember" is used for the spectral reference definition.

Nevertheless, the definition of endmembers should be carried out concerning the later utilization of these reference spectra, either for algorithms for a material detection (e.g. SAM) or for unmixing analysis (e.g. MTMF). For unmixing approaches, several autonomous endmember selection approaches like the Manual Endmember Selection Tool (MEST) (ii), the Pixel Purity Index (PPI), implemented in ENVI (iii) or the NFIND-R (iv) have been developed. These well-known algorithms detect pixel in hyperspectral image data, that define the convex hull of a point cloud in the corresponding spectral n-dimensional feature space.

However, algorithms for material detection purposes, like SAM, determine the spectral similarity between a pixel's spectra and a given endmember. In contrast to endmembers for spectral unmixing, which often represent 'spectral extreme' features, algorithms like SAM require endmember containing the 'mean spectra' of a material class in order to produce best possible results between classes with a similar spectral behaviour. The determination of reference spectra as an endmember for material detection approaches like SAM could be carried out by measurements in situ with a field spectrometer or by a selection of pixels in the image data. The objective of this work is the development and implementation of an unsuperivised image endmember definition process.

METHODS

Determination of Endmember Candidates

As a first step of the presented approach, all image pixels that could become an image endmember have to be determined. A pixel in the hyperspectral data, that contains the reflectance spectrum of a homogenous surface is a *candidate* for a material definition. Due to the relatively coarse spatial resolution of imaging spectrometers (e.g. GSD of > 3 m), the image data contains a lot of pixel with mixed spectra. These pixel are mostly located at the border between two surfaces with different spectral features. If the geometry of these objects is known, these mixed pixels could be filtered out and disregarded in further processing. In a multisensor environment, spatial high resolution image data could be segmented in order to retrieve this necessary geometry information. In this study, the image segments were derived by use of a region growing segmentation technique, the Fractal Net Evaluation Approach (FNEA) (v) which is implemented in the software eCognition.

By superimposing the image segments of the orthophoto on the hyperspectral image data, pixel in the hyperspectral image, that are completely (within N4 or N8 neighborhood, see Figure. 1) included in these segments, are marked as candidates for an endmember definition.

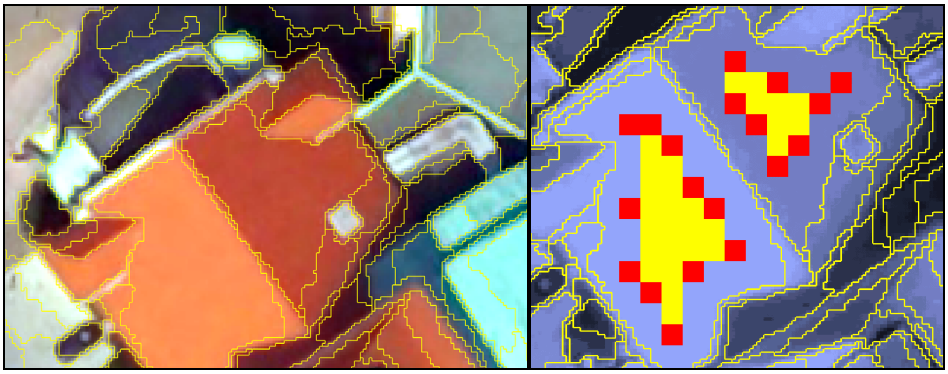

Figure 1: Segments of an orthophoto (left) are used to determine candidate-pixel in the hyperspectral image data. On the right side, N8-filtered candidates are shown in yellow, N4 filtered are additionally coloured in red.

In further processing steps of the presented approach, the endmember candindates will be joined into groups with similar spectral behaviour. The separation of different groups and the combination of spectral similar image pixel to an endmember depends on the candidate's spectral features. The geometric information (link between candidate and segment) is not used in the following approach. As a consequence, invalid image segments containing different material spectra have no influence on the following definition process.

Measuring spectral similarity

After the definition of a set of endmember candidates by a GIS-overlay operation as described above, the member of this set have to be clustered by their spectral similarity. For distance based clustering approaches, a feature space is necessary to determine the proximity matrix between all objects to cluster. For the presented approach, a feature space is developed, that expresses the spectral similarity between the candidates as effective as possible.

In a first approach, the original spectral feature space was taken into account. However, in some cases like urban studies the spectra of reference materials are often a result of a spectral mixture of different (manmade) materials. As a result, this mixture leads to flat spectral features, or, in addition, some of these materials have similar spectral features and are hardly separable in an original or transformed feature space, as shown in Figure 2.

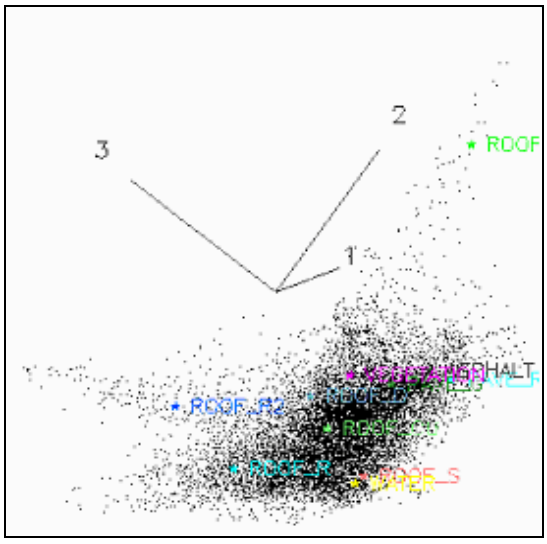

Figure 2: Image endmembers of urban materials in a MNF feature space (first three axes).

Deterministic approaches like SAM allow the construction of an advanced feature space for the separation of spectral similar candidates. The following matrix is an example for the estimation of the spectral angle between 23 endmember candidates in an urban environment. As shown in figure 3, the spectral angle is calculated for each candidate regarding to the other 22 candidates left in the set. A first view to the SAM-matrix in Figure 3 shows five distinct groups of candidates.

1	0,00	0,11	0,03	0,70	0,69	0,69	0,69	0,53	0,54	0,53	0,53	0,40	0,40	0,39	0,38	0,38	0,61	0,63	0,49	0,50	0,50	0,51	0,51
2	0,11	0,00	0,13	0,72	0,71	0,71	0,71	0,55	0,55	0,55	0,54	0,40	0,40	0,39	0,39	0,39	0,61	0,62	0,49	0,50	0,50	0,51	0,51
3	0,03	0,13	0,00	0,69	0,69	0,69	0,69	0,53	0,53	0,53	0,53	0,40	0,40	0,40	0,39	0,39	0,62	0,63	0,49	0,50	0,50	0,51	0,51
4	0,70	0,72	0,69	0,00	0,00	0,01	0,01	0,18	0,18	0,18	0,18	0,34	0,34	0,35	0,35	0,35	0,23	0,23	0,25	0,25	0,25	0,25	0,25
5	0,69	0,71	0,69	0,00	0,00	0,01	0,00	0,17	0,17	0,17	0,18	0,33	0,34	0,34	0,35	0,34	0,23	0,23	0,25	0,25	0,25	0,25	0,25
6	0,69	0,71	0,69	0,01	0,01	0,00	0,01	0,18	0,17	0,17	0,18	0,34	0,34	0,35	0,35	0,35	0,23	0,23	0,25	0,25	0,25	0,25	0,25
7	0,69	0,71	0,69	0,01	0,00	0,01	0,00	0,17	0,17	0,17	0,18	0,33	0,34	0,34	0,35	0,34	0,23	0,23	0,25	0,25	0,25	0,25	0,25

Figure 3: First seven Rows of a matrix with spectral angles of 23 candidates. Row one, column two is the angle (0,11) between candidate one and candidate two.

This matrix can also be viewed as a 23-dimensional feature space. By defining the first row a x-axis, the second as y-axis and the third as z-axis, a new feature space can be created (see Figure 3, left).

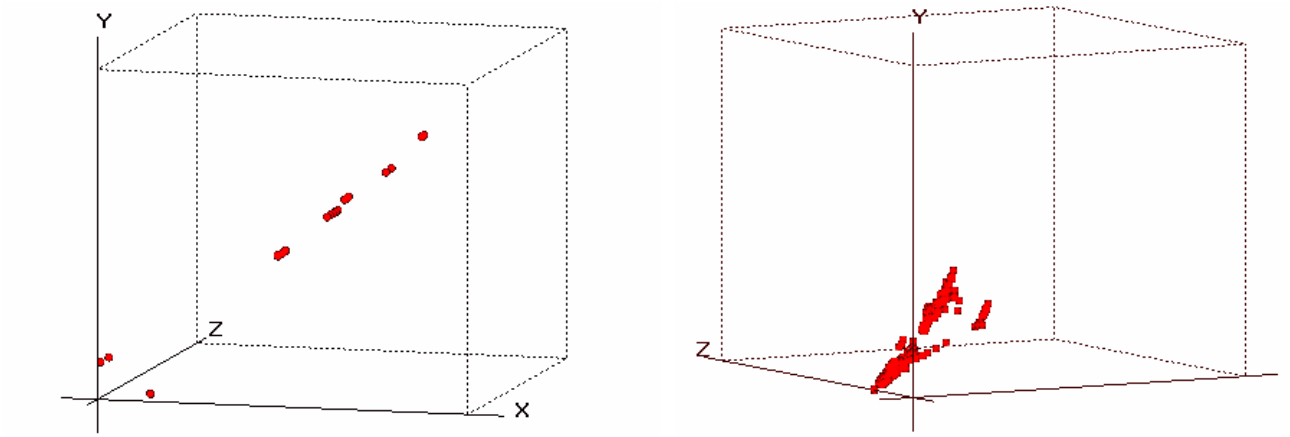

Figure 4: 3-D feature space spawned by the rows of a SAM-matrix. Left: 23 candidates of the SAM-matrix, shown in Figure 3 and an example with over 600 candidates (right).

The feature space on the left side of Figure 4 shows seven distinct clusters. The high correlation between the candidates is obviously visible. With a higher number of candidates, some clusters are connected, although the ten given materials for this example are clearly distinctive (Figure 4 right).

The correlation coefficient is another deterministic approach for the estimation of a spectral similarity. The correlation coefficient allows a more precise differentiation of spectral similar materials (vi). This technique is also used in classification approaches like CCSM (vii) and pattern recognition in hyperspectral image data (viii).

The given reflectances r_{ij} of a pixel $p_{j:}$

$$p_j = \sum_{i=1}^{n} r_{ij}$$

are transformed by substracting the mean value of r_j and normalizing to the sum of one, so that the spectra have the following characteristics:

$$\sum_{i=1}^{n} a_i = 0 \qquad \sum_{i=1}^{n} a_i^2 = 1$$

The correlation coefficient c_jk between spectrum a_{ij} and a_{ik} could be estimated by:

$$c_j k = \sum_{i=1}^{n} a_{ij}\ a_{ik}$$

The calculation of the correlation coefficient between n candidates results in a n x n correlation matrix. The rows of the correlation matrix can be used as the definition of the coordinate-axis of a new feature space (see Figure 5).

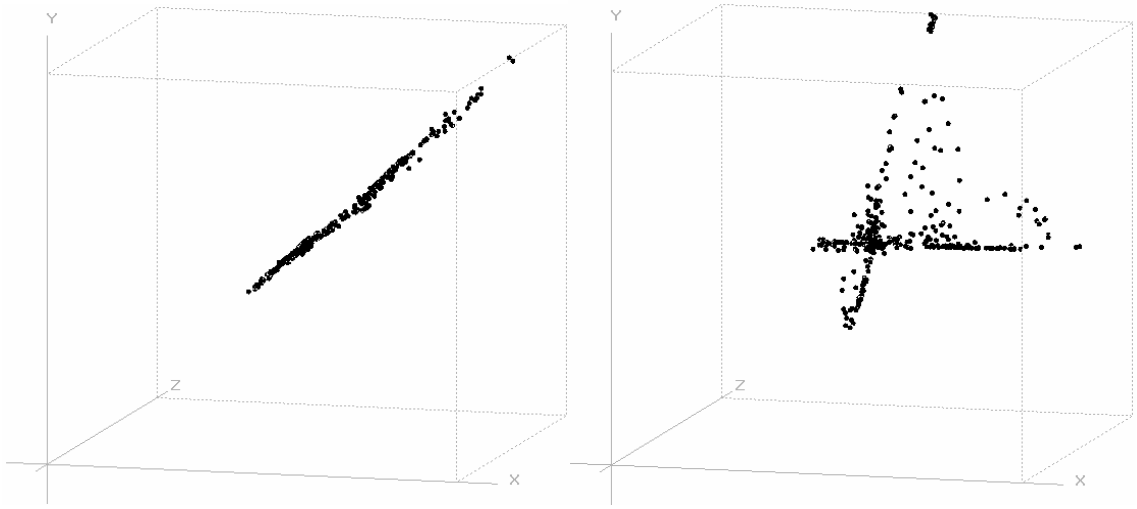

Figure 5: Rows of a correlation matrix as feature space which is highly correlated.The first three of a correlation matrix of 444 candidates are displayed on the left. A different selection of rows (1,3 and 13) lead to different visualization (right).

The seperability of candidates in the feature space is highly depending on the selection of rows from the correlation matrix, that define the axis of the new feature space. Additionally, the data shows a high correlation. As a consequence, a Principal Component Analysis (PCA) is carried out within the complete correlation matrix data. The result is a PCA-transformed correlation matrix with rows sorted by the eigenvalues of the PCA. The rows of this transformed matrix can also be used as definition for the coordinate axes of a n-dimension feature space (see Figure 6).

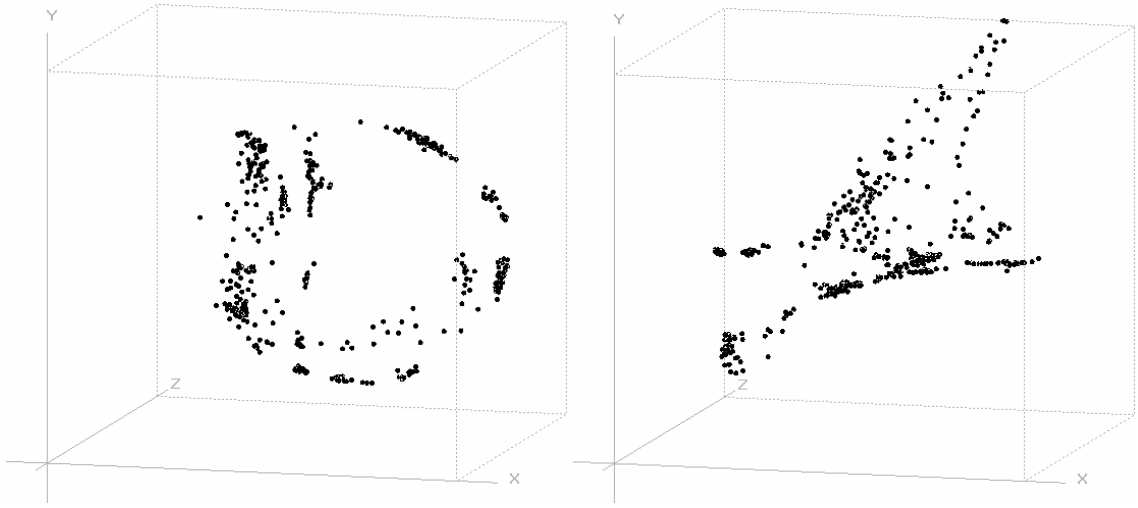

Figure 6: Feature space, resulting from a PCA-transformed correlation matrix. Left: axis of feature space defined by the first three PCA-components, higher PCA-components (3,5 and 7) still contain data (right image).

Clustering of similar spectra

Candidates in the PCA-transformed feature space build drawn-out linear point clouds (Figure 6). The well-known clustering algorithms like k-means or ISODATA offer no solution to sepereate distinct clusters having such drawn-out shapes. Therefor, in this paper, the density based clustering algorithm (also known as DBSCAN) is used to cluster the candidates. The central concept of DBSCAN is the estimation of a ‘density’ of a point neighborhood.

A radius, representing the neighborhood of a point is predefined by the user. This neigborhood has to contain at least a minimum number of points in order to build a cluster. The radius and the number of points in the given neighborhood are the two threshold values defining the 'density' of a cluster (Figure 7).

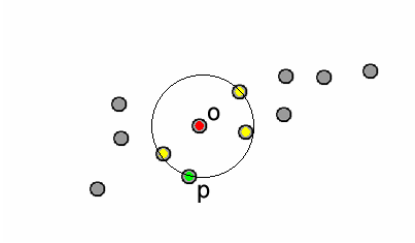

*Figure 7: For a given radius and a minimum numbers of reachable neighbor points, point **O** is a core object of a new cluster including neighbor points like **P**.*

In further iterations, reachable neighbors are successive included into the cluster. Based on this strategy, point clouds with drawn-out shapes could be clustered (Figure 8).

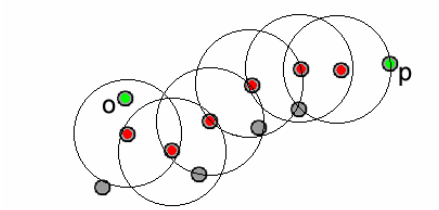

*Figure 8: The points **O** and **P** belong to the same cluster, connected through the core objects (displayed in red).*

As described above, the DBSCAN algorithm depends on two thresholding parameters. The radius and the minimum number of neighbor points has to be fixed by the user. For this study, the radius is estimated by the mean minimum distance to the next neighbor over all points in the dataset. The only remaining parameter fixed by the user is the number of neighbors, which was fixed in a range of 1 to 3 for this study. The results of the described clustering algorithm is shown in the following figure.

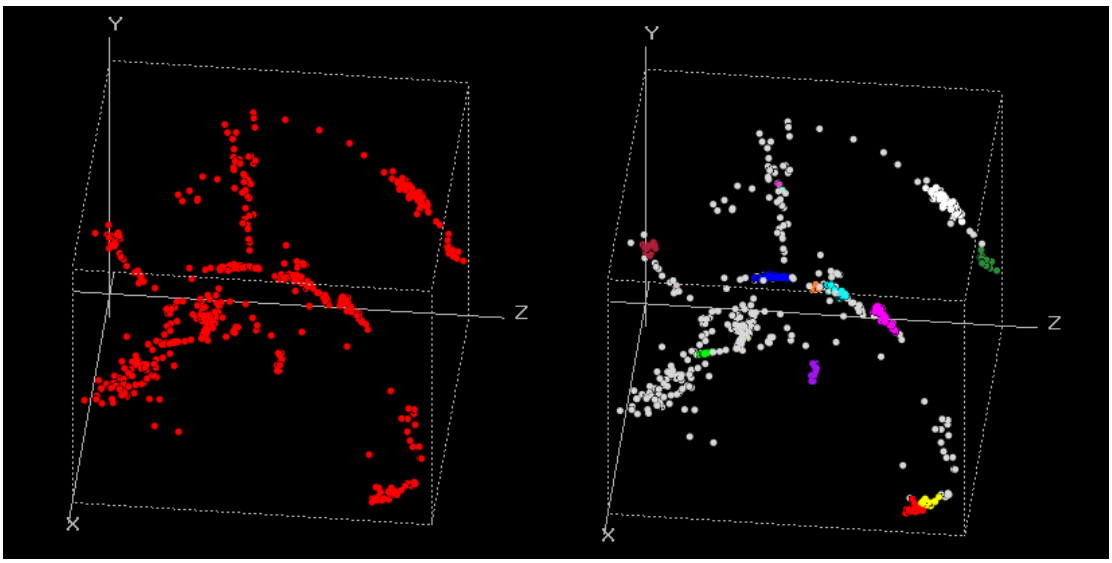

Figure 9: Unclustered point cloud (left) and the first 16 cluster generated by DBSCAN (right).

Building the spectral library

DBSCAN provides for each candidate a Cluster-ID. In case of a successfull clustering, a candidate retrieves the ID of the assigned cluster. A negative ID (-1) indicates those candidates, who are not assigned to any cluster. As a result of the clustering process, a mask image with the same extent as the hyperspectral image data contains these Cluster-IDs at the geometric location of each candidate. Pixel with the same ID (member of one Cluster) could be joined to one group (region of interest). Averaging the corresponding spectra of such a group in the hyperspectral dataset leads to a reference spectra.

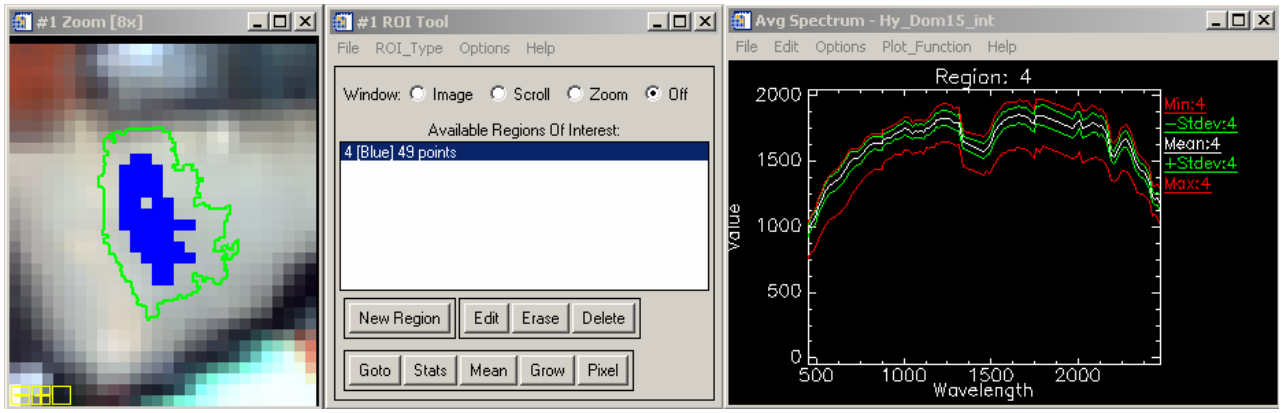

Figure 10: Image pixel, grouped by their cluster ID on the left lead to a group of 49 pixel (middle). The average spectrum of this group and statistical parameters (min, max, stddev on the right side) can be estimated by use of standard-software.

RESULTS

As a proof of principle, the proposed method is used to detect ten different known materials in an urban test site (500 m x 1000 m). After an image segmentation of an orthophoto, covering the whole scene, a subset of image segments with six known ground materials and four known roofing materials was used to estimate the set of endmember candidates. 753 candidates were detected and clustered by DBCSAN. The first 16 cluster were stored in a spectral library, the statistical properties of the reference spectra are shown in the following table.

Table 1: The first 16 Clusters and their statistical properties.

Cluster	# of Pixel	stddev	Material	Cluster	# of Pixel	stddev	Material
1	101	1,1 %	granite (pavement)	9	22	16,5 %	zinc
2	79	7,5 %	clay (roofing red)	10	21	1,1 %	copper
3	51	0,5 %	granite (pavement)	11	57	0,3 %	water
4	58	5,3 %	Vegetation	12	16	0,5 %	concrete
5	47	11,2 %	concrete rooftop	13	16	0,3 %	clay pavement
6	48	5,3 %	clay (roofing dark)	14	10	0,3 %	water/vegetation
7	57	4,1 %	Copper	15	9	4,2 %	clay (roofing red)
8	59	3,8 %	asphalt/bitumen	16	7	0,3 %	gravel

All ten known materials were detected within the above displayed 16 clusters. Some material cluster like granite (cluster 1 and 3) and red clay roofing material (cluster 2 and 9) were not correctly

joined. However, the high standard deviation of some roofing materials (e.g. cluster 5 with 11,2%) shows, that this method is basically able to join image pixel with different surface slope or aspect.

CONCLUSION

The presented algorithm for an unsupervised endmember selection shows first promising results. A reliable transformation method from the original spectrum to a feature space that expresses the similarity of spectra has been developed. The following density based clustering lead to useful pixel groups, which average spectra can be stored in a spectral library. Future steps will be the development of a framework application to assist the user for quality assessment and a vsiual control on the clustering process.

Finally, by use of this approach, the user has only to examine the results of the clustering process and to join some clusters manually, if necessary. The manual selection of image pixel for a certain material is replaced by this approach.

REFERENCES

i A. Greiwe and M. Ehlers, 2005: Combined analysis of hyperspectral and high resolution image data in an object oriented classification approach. In: Proceedings of 3rd International Symposium on Remote Sensing and Data Fusion over Urban Areas 13-15 March 2005, Phoenix(Arizona), USA.

ii Bateson and Curtiss, 1996: A Method for manual endmember Selection and Spectral Unmixing, Remote Sensing and Environment (55), pp. 229–243.

iii J. W. Boardman, F. A. Kruse, and R. O. Green 1995: Mapping target signatures via partial unmixing of aviris data. In: Summaries, Fifth JPL Airborne Earth Science Workshop, JPL Publication 95-1 (1), pp. 23–26.

iv M. E. Winter 1999: Fast autonomous spectral endmember determination in hyperspectral data, Proceedings of the Thirteenth International Conference on Applied Geologic Remote Sensing (II), pp. 337 – 344.

v Baatz, M. und Schäpe, A., 1999: Object-oriented and multi-scale image analysis in semantic networks. In: Proc. of the 2nd International Symposium on Operationalization of Remote Sensing, Enschede, ITC.

vi de Carvalho Jr, O. A., de Carvalho, A. P. Ferreira und Meneses, P. R., 2000: Sequential minimum noise fraction use: An approach to noise elimination. In: Summaries of the Ninth Annual JPL Airborne Earth Science Workshop. JPL Pub 00-18.

vii van der Meer, F. und Bakker, W., 1997: CCSM: Cross correlogram spectral matching. In: International Journal of Remote Sensing, Band 18:S. 1197–1201.

viii Ingram, R. N., Lewis, A. S. und Tutweiler, R. L., 2004: An automatic nonliear correlation approach for processing of hyperspectral images. In: International Journal of Remote Sensing, Vol 25(20): pp. 4981–4998.